

Tiankai Xie, Caleb Geniesse, Jiaqing Chen, Yaoqing Yang, Dmitriy Morozov, Michael W Mahoney, Ross Maciejewski, and Gunther H Weber. Evaluating loss landscapes from a topology perspective. *arXiv preprint arXiv:2411.09807*, 2024.

Jingkang Yang, Kaiyang Zhou, Yixuan Li, and Ziwei Liu. Generalized Out-of-Distribution Detection: A Survey, 2022a.

Yaoqing Yang, Liam Hodgkinson, Ryan Theisen, Joe Zou, Joseph E Gonzalez, Kannan Ramchandran, and Michael W Mahoney. Taxonomizing local versus global structure in neural network loss landscapes. *Advances in Neural Information Processing Systems*, pages 18722–18733, 2021.

Yaoqing Yang, Ryan Theisen, Liam Hodgkinson, Joseph E Gonzalez, Kannan Ramchandran, Charles H Martin, and Michael W Mahoney. Evaluating natural language processing models with generalization metrics that do not need access to any training or testing data. *arXiv preprint arXiv:2202.02842*, 2022b.

Zhewei Yao, Amir Gholami, Kurt Keutzer, and Michael W Mahoney. PyHessian: Neural networks through the lens of the hessian. In *2020 IEEE international conference on big data (Big data)*, pages 581–590. IEEE, 2020.

Yefan Zhou, Yaoqing Yang, Arin Chang, and Michael W Mahoney. A three-regime model of network pruning. In *International Conference on Machine Learning*, pages 42790–42809. PMLR, 2023.

Appendix A. Visualizing Different Physical Constraints

In Figure A.5, we show topological landscape profiles for two different random initializations (from left to right) of a physics-informed neural network (PINN). Note, that the landscapes look different for the different random initializations because we are looking at a model corresponding to the transition from low to high error. Overall the global shape of the topological landscape profile looks similar when comparing the same random seed across three- and four-dimensional loss landscapes. In four dimensions, we observe many more critical points and that the basins in the much spikier landscape can be mapped back to the wider basins in the topological landscape profiles based on the three-dimensional loss landscapes. These visualizations also highlight an important feature of our topological landscape profile representations—the ability to visualize higher-dimensional loss landscapes.

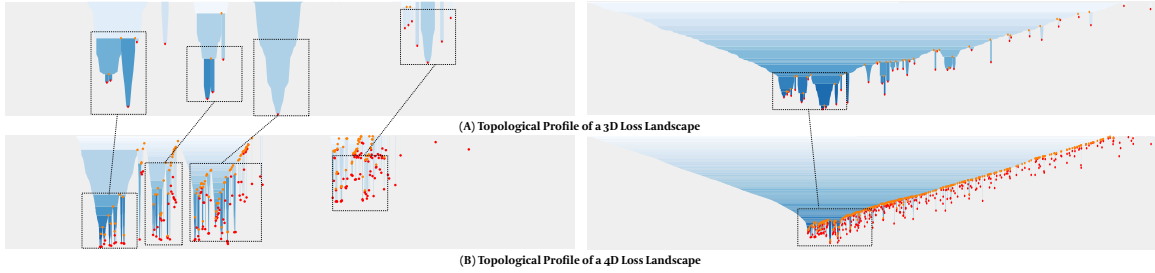


Figure 5: Comparing topological landscape profiles based on (A) three-dimensional and (B) four-dimensional loss landscapes. See Section 4.1 for details.

Appendix B. Visualizing Loss Landscapes Over Training

In Figure B.6, we show how the loss landscape changes across different learning rates. When looking at the loss landscapes for three different random seeds, after zooming in, we observe consistent variation in the depth and shape of the loss landscape as the learning rate is varied. See Section 4.2 for details.

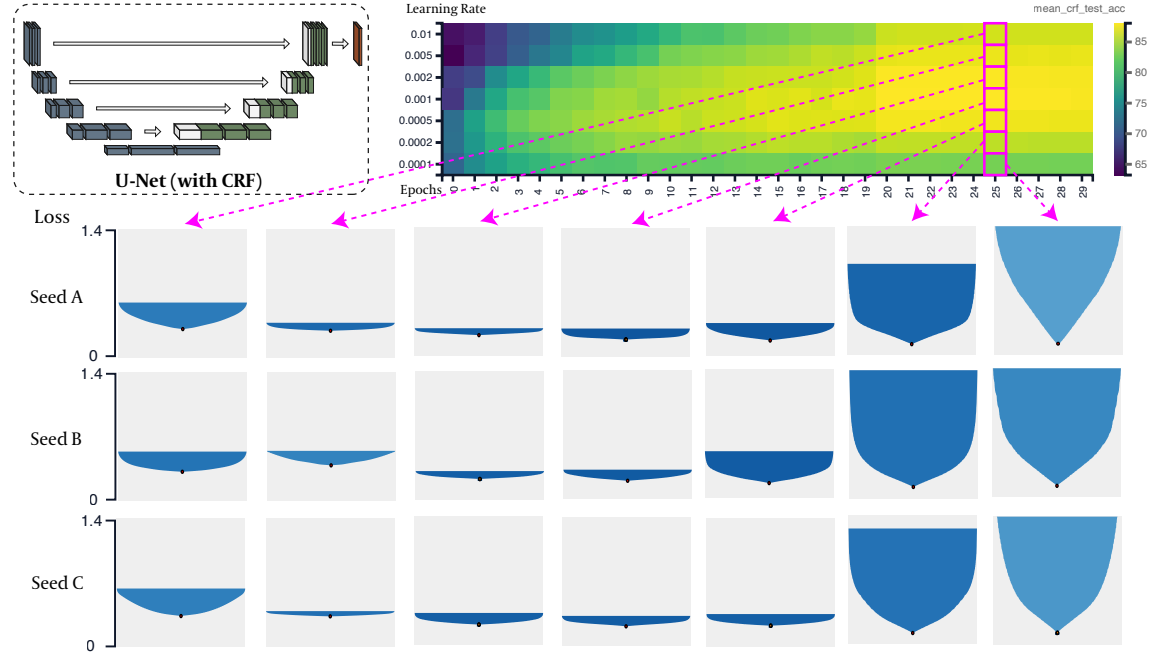


Figure 6: Loss landscapes across learning rates for UNet models with a CRF layer trained on the Oxford-IIIT Pet dataset. See Section 4.2 for details.